Physiol Genomics 48: 826–834, 2016.
First published September 23, 2016; doi:10.1152/physiolgenomics.00089.2016.

CALL FOR PAPERS | *Gut Microbiota in Health and Disease*

Microbial short chain fatty acid metabolites lower blood pressure via endothelial G protein-coupled receptor 41

Niranjana Natarajan,[1] Daijiro Hori,[2] Sheila Flavahan,[2] Jochen Steppan,[2] Nicholas A. Flavahan,[2] Dan E. Berkowitz,[2] and Jennifer L. Pluznick[1]

[1]*Department of Physiology, Johns Hopkins University, School of Medicine, Baltimore, Maryland; and* [2]*Department of Anesthesiology and Critical Care Medicine, Johns Hopkins University, School of Medicine, Baltimore, Maryland*

Submitted 27 July 2016; accepted in final form 19 September 2016

Natarajan N, Hori D, Flavahan S, Steppan J, Flavahan NA, Berkowitz DE, Pluznick JL. Microbial short chain fatty acid metabolites lower blood pressure via endothelial G protein-coupled receptor 41. *Physiol Genomics* 48: 826–834, 2016. First published September 23, 2016; doi:10.1152/physiolgenomics.00089.2016.—Short chain fatty acid (SCFA) metabolites are byproducts of gut microbial metabolism that are known to affect host physiology via host G protein-coupled receptor (GPCRs). We previously showed that an acute SCFA bolus decreases blood pressure (BP) in anesthetized mice, an effect mediated primarily via Gpr41. In this study, our aims were to identify the cellular localization of Gpr41 and to determine its role in BP regulation. We localized Gpr41 to the vascular endothelium using RT-PCR: Gpr41 is detected in intact vessels (with endothelium) but is absent from denuded vessels (without endothelium). Furthermore, using pressure myography we confirmed that SCFAs dilate resistance vessels in an endothelium-dependent manner. Since we previously found that Gpr41 mediates a hypotensive response to acute SCFA administration, we hypothesized that Gpr41 knockout (KO) mice would be hypertensive. Here, we report that Gpr41 KO mice have isolated systolic hypertension compared with wild-type (WT) mice; diastolic BP was not different between WT and KO. Older Gpr41 KO mice also exhibited elevated pulse wave velocity, consistent with a phenotype of systolic hypertension; however, there was no increase in ex vivo aorta stiffness (measured by mechanical tensile testing). Plasma renin concentrations were also similar in KO and WT mice. The systolic hypertension in Gpr41 KO is not salt sensitive, as it is not significantly altered on either a high- or low-salt diet. In sum, these studies suggest that endothelial Gpr41 lowers baseline BP, likely by decreasing active vascular tone without altering passive characteristics of the blood vessels, and that Gpr41 KO mice have hypertension of a vascular origin.

microbiota; hypertension; GPCR; endothelium; acetate; propionate

THE ROLE OF COMMENSAL MICROBIOTA in modulating host physiology is a rapidly emerging and expanding concept. Microbial cells comprise a significant component of human physiology (36), and changes in the composition of the microbiota have been correlated with an array of pathophysiological processes, including cardiovascular disease and hypertension (5–7, 16, 20, 21, 31, 33). One of the well-characterized classes of gut microbial metabolites are short chain fatty acids (SCFAs), which are produced by the breakdown of dietary fiber in the colon (10, 12, 37). Although SCFAs are found in the μM to low mM range in the plasma, they are virtually undetectable in germ-free animals lacking commensal microbiota (29), indicating that the gut microbiota are the sole source of circulating SCFAs. Recent studies have found that SCFAs produced by the gut microbiota modulate host physiology by acting as ligands for host G protein-coupled receptors (GPCRs), including Gpr41, Gpr43, Olfr78, and Gpr109a (2, 11, 18, 23, 30, 31, 35). Previously, we reported that Olfr78 and Gpr41 differentially modulate blood pressure (BP) in response to acute delivery of SCFAs (31). We found that Olfr78 increases BP upon activation, at least in part by stimulating renin secretion from the juxtaglomerular apparatus. In addition, we reported that Olfr78 KO mice are hypotensive and that Olfr78 localizes to vascular smooth muscle cells (vSMCs) (31). In contrast, activation of Gpr41 decreases BP, as demonstrated by an altered acute dose response of BP to SCFAs in Gpr41 knockout (KO) mice (30, 31). As our prior studies were focused on Olfr78, our goal in this study was to better understand the role of Gpr41 in BP regulation and to test the hypothesis that Gpr41 KO mice are hypertensive.

In this study, we report that Gpr41 localizes to the vascular endothelium, in contrast to Olfr78, which is found in the vascular smooth muscle. We also demonstrate that the vascular endothelium is essential for SCFA-mediated vasodilation to occur, as vasodilation is absent in endothelium-denuded vessels ex vivo. To determine the role of Gpr41 in chronic BP regulation, we examine BP in Gpr41 KO and Gpr41 wild type (WT) by telemetry and reveal that Gpr41 KO mice exhibit isolated systolic hypertension, which is not salt sensitive. Thus, the present study suggests a novel role for Gpr41 in the endothelium to influence BP regulation. SCFA receptors expressed in both the vascular endothelium (Gpr41) and vascular smooth muscle (Olfr78) form a complex network to regulate BP in response to signals produced by the microbiota. In the future, better understanding of these pathways has the potential to further our understanding of BP regulation as a whole, as well as to more fully uncover the unique role of the gut microbiota in regulating both BP and vascular tone.

MATERIALS AND METHODS

RT-PCR from murine aorta. To localize Gpr41, we utilized RT-PCR. Thoracic aortas were dissected from 3 mo old C57BL/6 male mice, and total RNA was extracted using Qiagen RNeasy Mini kit with DNase digest performed before elution. To remove endothelium, thoracic aortas were sliced open longitudinally, and the endothelium was mechanically denuded before RNA extraction was performed. RNA was

Address for reprint requests and other correspondence: J. L. Pluznick, 725 No. Wolfe St., WBSB 205, Baltimore, MD 21205 (e-mail: jpluznick@jhmi.edu).

reverse transcribed using Bio-Rad iScript reverse transcriptase kit (random primers). Primer sequences for Gpr41, endothelial nitric oxide synthase (eNOS), and β-actin are given in Table 1. In a subset of samples, reverse transcriptase was omitted from the RT reaction (mock RT) as a negative control. PCR was carried out using Invitrogen Platinum Taq Mastermix for 35 cycles; all PCR products were sequenced to confirm.

Ex vivo vasoreactivity experiments. We euthanized 3 mo old C57BL/6 WT male mice by CO_2 asphyxiation. Proximal segments of the tail artery were dissected rapidly and placed in cold Krebs-Ringer bicarbonate solution containing 118.3 mM NaCl, 4.7 mM KCl, 1.2 mM $MgSO_4$, 1.2 mM KH_2PO_4, 2.5 mM $CaCl_2$, 25.0 mM $NaHCO_3$, and 11.1 mM glucose (control solution). The tail arteries (either intact or with endothelium denuded) were cannulated at both ends with glass micropipettes, secured by 12-0 nylon monofilament suture, and placed in a microvascular chamber (Living Systems, Burlington, VT) (4, 26). The arteries were maintained at a constant transmural pressure (P_{TM}) of 60 mmHg in the absence of flow. The chamber was superfused with control solution, maintained at 37°C, pH 7.4, and gassed with 16% O_2/5% CO_2/balance N_2. The chamber was placed on the stage of an inverted microscope (×20, Nikon TMS-F) connected to a video camera (CCTV camera, Panasonic). The vessel image was projected on a video monitor, and the internal diameter was continuously determined by a video dimension analyzer (Living Systems Instrumentation) and was monitored on a BIOPAC (Santa Barbara, CA) data acquisition system.(4, 26) The tail vessels were allowed to equilibrate at P_{TM} of 60 mmHg for 30 min. After equilibration, the vessels were constricted with phenylephrine to 80% of the baseline diameter and subsequently treated with increasing doses of sodium propionate and sodium acetate in the superfusate, and the internal diameters of the vessels were recorded over time. After propionate treatment, the reactivity of the vessels (and presence/absence of endothelium) was confirmed by acetylcholine.

Animals. Mice were housed in accordance with institutional, state, and national guidelines. All experimental protocols were approved by the Johns Hopkins University Institutional Animal Care and Use Committee (accredited by the Association for Assessment and Accreditation of Laboratory Animal Care International). Gpr41 KO [a kind gift from Drs. Yanagisawa (UT Southwestern) and Gordon (Washington University)](35) were backcrossed onto a C57BL/6 background, and Gpr41 heterozygotes were then bred in-house to obtain Gpr41 KO and Gpr41 WT littermates. All animals were given unrestricted access to food and water throughout the duration of the experiments. All animals were maintained on Teklad 2018SX, 18% protein diet, unless otherwise mentioned.

Chronic BP measurement. DSI TA11 PA-C10 devices were used to measure BP by radiotelemetry in 3 mo old male Gpr41 KO and WT mice. Catheters of the telemetry devices were inserted into the right carotid artery, and the radiotransmitter was localized subcutaneously in the abdomen. The procedure was performed under 2% isoflurane anesthesia, and the mice were allowed 7 days for recovery. BP was recorded continuously in the implanted mice after recovery. A 5-day recording period was used to assess baseline BP. Systolic, diastolic, pulse pressure, and heart rate were averaged through this period.

Table 1. *PCR primer sequences*

Gpr41, 685 bp	
Fwd:	ACGGCGGTGAGCATCGAACG
Rev:	TTCCACCCCCTCCTGCGGTC
β-Actin, 353 bp	
Fwd:	GCTCGTCGTCGACAACGGCTC
Rev:	CAAACATGATCTGGGTCATCTTCTC
eNOS, 230 bp	
Fwd:	CTGCTGCCCGAGATATCTTC
Rev:	CTGGTACTGCAGTCCCTCCT

Gpr41, G protein-coupled receptor 41; eNOS, endothelial nitric oxide synthase; Fwd, forward; Rev, reverse.

Animals were maintained on Teklad 2018SX, with 18% protein, during this experimental duration.

Pulse wave velocity. Pulse wave velocity (PWV) was measured noninvasively in 3 mo old and 6 mo old male Gpr41 KO and WT mice with a high-frequency, high-resolution Doppler spectrum analyzer (DSPW; Indus Instruments, Houston, TX). Under anesthesia with 1.5% isoflurane, mice were placed in a supine position on a temperature-controlled platform, equipped with EKG. Core temperature was maintained at 37°C, and the heart rate was allowed to stabilize to a physiological range. Subsequently, a 20 MHz probe was used to measure flow velocities in the descending aorta and abdominal aorta. A real-time signal acquisition and spectrum analyzer system was used to calculate the time between the R wave of EKG to the start of pulse wave form for each measurement location (3).

Tensile testing of Gpr41 aorta. Aortas from 6 mo old Gpr41 male mice were harvested and cut into 2 mm rings and mounted on the pins of an electromechanical puller (DMT560; Danish Myo Technology, Aarhus, Denmark). After calibration and alignment, the pins were slowly moved apart with an electromotor at a rate of 20 μm/s to apply radial stress on the specimen until breakage. Force and displacement were continuously recorded. A 1 mm segment proximal to the ring was imaged at a ×10 magnification. The inner and outer diameters of the vessel were measured at four locations using Image J software [National Institutes of Health (NIH), Bethesda, MD]. Average inner and outer diameters were used to calculate sample thickness. Engineering stress (S) was calculated by normalizing force (F) to the initial area of the specimen: $S = F/2tl$, where t = thickness and l = length of the sample. Engineering strain (λ) was calculated as the ratio of displacement to initial diameter. The stress-strain relationship was represented by the equation $S = \alpha e^{\beta\lambda}$ where α and β are constants, determined by nonlinear regression for each sample (38). A subset of aortas were decellularized; for this, aortas from Gpr41 KO and WT mice were incubated in decellularization *solution 1* (8 mM CHAPS, 1 M NaCl, and 25 mM EDTA in PBS) for 44 h. Next, samples were incubated in decellularization *solution 2* (1.8 mM sodium dodecyl sulfate, 1 M NaCl, 25 mM EDTA in PBS) for 44 h. The decellularization solutions were changed every 22 h with three 15 min PBS washes. After incubation in decellularization solutions, aorta segments were washed and incubated in PBS for 2 days to remove residual detergents. All steps were conducted at room temperature under constant shaking. Finally, samples were incubated at 37°C for 1 day in endothelial cell media (ScienCell Research Labs) and washed thrice in PBS for 15 min each, to obtain decellularized specimen. These aortas were then analyzed (tensile testing) as described above.

Plasma analysis. Blood chemistry of 3 mo old male and female Gpr41 mice was analyzed using iSTAT Chem8+ cartridge with handheld iSTAT system using samples taken from the superficial temporal vein. Histological analyses of blood vessels were conducted on aortas excised from 6 mo old mice killed by CO asphyxiation. Aortas were stained with picrosirius red for quantifying total collagen amount and Verhoeff's van Gieson stain to quantify elastin. Images obtained from the stained aorta sections were quantified using ImageJ (NIH). Plasma renin concentration was measured in 3 mo old mice with a modified angiotensin I measurement kit (Peninsula Labs S-1180). Prior to starting the assay, plasma was diluted 15-fold and incubated with excess porcine angiotensinogen (Sigma SCP0021) for 20 min at 37°C in a buffer containing 50 mM sodium acetate (pH 6.5), 10 mM AEBSF, 10 mM EDTA (pH 8.0), 1 μM porcine angiotensinogen, and 10 mM 8-hydroxyquinoline. After incubation with angiotensinogen, the samples were analyzed according to the protocol provided with the kit. Plasma renin concentration was assayed by competitive binding of angiotensin 1 generated to its antibody (32). For both plasma renin and plasma electrolytes, data are presented with sexes combined as no sex differences were observed.

Sodium loading studies. For sodium loading studies, mice were implanted with radiotransmitters to record blood pressure and maintained on a different control diet (0.49% NaCl, TD.96208), and blood

pressure was recorded for 5 days. This was followed by 7 days on a matched high-salt diet (4% NaCl, TD.92034) and 5 days on a low-salt diet (0.01% NaCl, TD.90228).

RESULTS

Gpr41 localizes to the vascular endothelium. Studies have reported that Gpr41 is expressed in a variety of tissues including the heart, lungs, and sympathetic nervous system (2, 13, 20, 31, 40, 41, 43). We have previously shown that murine Gpr41 is expressed in major blood vessels by RT-PCR (31) and that Olfr78 (another SCFA receptor) localizes specifically to vSMC (30, 31). Commercially available antibodies for Gpr41 are unreliable in our hands (antibodies give similar staining in Gpr41 KO and Gpr41 WT mice and/or fail to recognize overexpressed Gpr41). Therefore, to determine whether Gpr41 also localizes to vSMC, we assayed for Gpr41 expression by RT-PCR both in intact blood vessels and in blood vessels from which the endothelium had been denuded. Although β-actin is robustly detected in both intact and denuded vessels, both eNOS (an endothelial marker) and Gpr41 are present in intact blood vessels, but not in blood vessels with denuded endothelium (Fig. 1*A*), indicating that Gpr41 localizes to endothelial cells.

SCFA-mediated vasodilation is dependent on the endothelium. It has been previously reported that SCFAs dilate vessels ex vivo (22), and we have proposed that this vasodilation underlies the acute hypotensive response to SCFAs. However, the literature is divided on whether this vasodilation is endothelium dependent. Because Olfr78 localizes to vSMCs, whereas Gpr41 is found in endothelial cells, we wanted to definitely determine (using both resistance blood vessels and physiological doses of SCFAs) whether the endothelium is required for SCFA-mediated vasodilation. To that end, we performed ex vivo experiments using isolated resistance vessels (4, 26, 44). SCFAs propionate and acetate induced vasodilation of tail arteries (Fig. 1), with a dose dependence that is similar to the hypotensive response in vivo (31). The vasodilation observed with both propionate and acetate was endothelium dependent (Fig. 1, *B* and *C*), as the vasodilation of denuded vessels is significantly attenuated. SCFA-mediated vasodilation was not inhibited in the presence of 0.1 mM L-NAME, indicating that SCFA-mediated vasodilation is mediated predominantly by an eNOS-independent mechanism (Fig. 1, *D* and *E*).

Gpr41 KO mice exhibit isolated systolic hypertension at baseline. Our previously published data imply that acute activation of Gpr41 lowers BP (31). Therefore, we hypothesized that Gpr41 KO mice would be hypertensive. To test this hypothesis, we used telemetry to measure baseline BP in Gpr41 WT and Gpr41 KO mice (~3 mo of age). Gpr41 KO mice exhibited isolated systolic hypertension at baseline (Fig. 2, *A* and *B*). The reported values (Fig. 2) represent averages from a 5-day recording of BP in 3 mo old male animals of both genotypes. Consistent with higher systolic pressures in the Gpr41 KO animals, the pulse pressures of Gpr41 KO were significantly elevated during both dark and light cycles (Fig. 2*C*). Mean arterial pressure was significantly higher in Gpr41 KO mice during the dark cycle only. There were no differences between genotypes for diastolic pressure or heart rate (Fig. 2, *A* and *D*), or for plasma electrolytes (Table 2).

Isolated systolic hypertension is associated with endothelial dysfunction and results from an increase in arterial stiffness (especially in larger arteries) (15, 42, 45). To assess blood vessel stiffness in vivo, we measured PWV in Gpr41 KO and

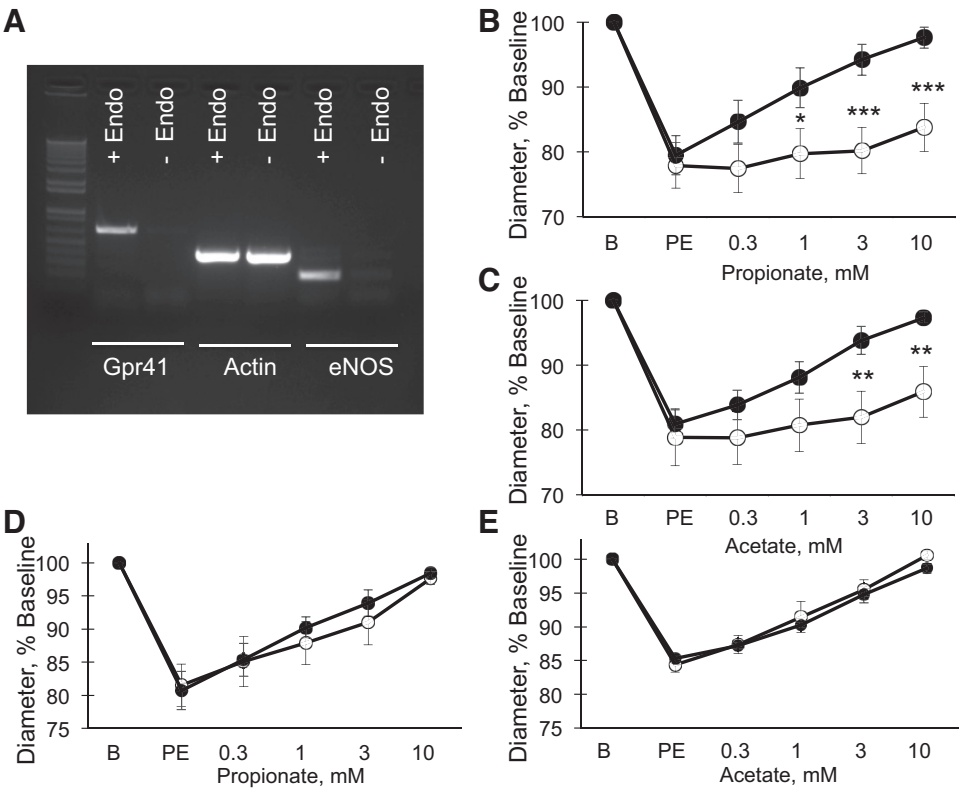

Fig. 1. G protein-coupled receptor (Gpr)41 is expressed in the endothelium, and short chain fatty acid (SCFA)-mediated vasodilation is endothelium dependent. *A*: Gpr41 localizes to the vascular endothelium by RT-PCR. eNOS (endothelial nitric oxide synthase), an endothelial marker, is detected in intact vessels (+endo) but not in vessels lacking endothelium (−endo). β-Actin, as a control, is detected in both +endo and −endo vessels. Gpr41, like eNOS, is only detected in intact vessels. In isolated tail arteries, both propionate (*B*) and acetate (*C*) cause endothelium-dependent vasodilation. Vessels with endothelium (●) exhibit vasodilation, which is severely attenuated when the endothelium is denuded (○), $n = 4$. L-NAME, a pharmacological inhibitor of eNOS does not attenuate SCFA-mediated vasodilation. Closed circles (no L-NAME) and open circles (0.1 mM L-NAME) exhibit similar vasodilation upon addition of propionate (*D*) and acetate (*E*). $n = 4$, $^{*}P < 0.05$, $^{**}P < 0.01$, $^{***}P < 0.001$. B, baseline; PE, phenylephrine.

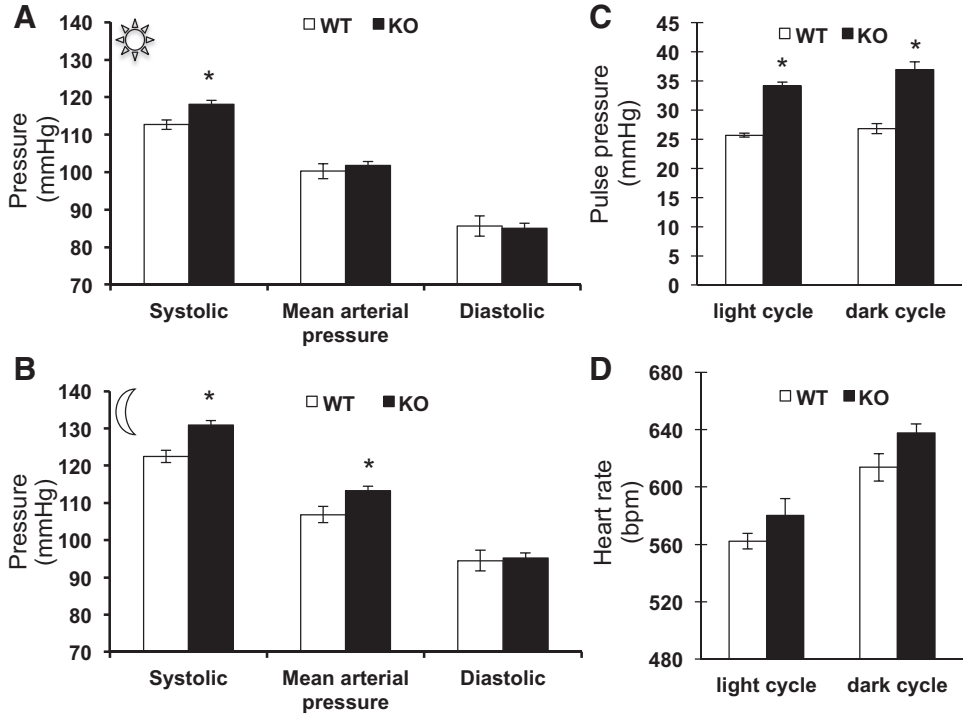

Fig. 2. Gpr41 knockout (KO) mice exhibit isolated systolic hypertension at baseline. Gpr41 KO mice have significantly higher systolic pressure during the light cycle (*A*) and dark cycle (*B*), higher mean arterial pressure during the dark cycle (*B*), but similar diastolic pressure during both dark and light cycle. Pulse pressures of Gpr41 KO mice are significantly elevated both during light and dark cycles (*C*); however, heart rate (*D*) is not altered. $n = 8$ KO, 6 wild type (WT); $^*P < 0.05$ between genotypes.

Gpr41 WT animals (28, 38). Although there were no genotypic differences at 3 mo of age, at 6 mo of age PWV was significantly elevated in Gpr41 KO compared with age-matched WT littermates (Fig. 3*A*). In contrast, tensile testing of aortas showed that the tensile properties of aortas from intact 6 mo old Gpr41 WT and Gpr41 KO aortas were comparable (similar compliance) (Fig. 3*B*), whereas the tensile properties of decellularized aortas from Gpr41 KO mice were significantly more compliant (Fig. 3*C*).

Chronic hypertension leads to vascular remodeling, resulting in the deposition of increased amounts of collagen in the arterial wall. This vascular fibrosis results in a thickening of the vessels and decreases their compliance (14). We analyzed the thickness and diameter of aortas from 6 mo old Gpr41 KO and WT mice and quantified the total amount of collagen and elastin in the aortas (Fig. 3, *D–G*). Consistent with the hypertensive phenotype observed in Gpr41 KO animals, Gpr41 KO aortas exhibited a significant increase in thickness, while the diameter was unaltered (Fig. 3, *D–G*). In addition, the collagen area fraction of Gpr41 KO aortas was significantly higher, and the thickness of the collagen layer trended toward an increase (Fig. 3, *F* and *G*). Interestingly, the total amount of elastin in Gpr41 KO aortas was also increased (Fig. 3, *E* and *G*), which might contribute to the increase in compliance of decellularized aortas observed in tensile testing studies of Gpr41 KO aortas (Fig. 3*C*). Heart-to-body weight ratios were higher in 6 mo old Gpr41 KO, whereas kidney-to-body weight ratios were similar between the two genotypes (Fig. 3*G*).

Plasma renin concentration. We previously reported that another SCFA receptor, Olfr78, modulates renin secretion from the juxtaglomerular apparatus (30, 31). To assess if Gpr41 KO mice had any compensatory changes in plasma renin, we measured plasma renin concentration in 3 mo old male and female Gpr41 KO and Gpr41 WT mice and found no genotypic differences (Table 3).

Gpr41 KO mice do not exhibit salt-sensitive hypertension. Dietary salt intake is a key contributing factor to hypertension. To determine if the isolated systolic hypertension in Gpr41 KO is salt sensitive, a separate cohort of age matched (~3 mo of age) Gpr41 KO and WT mice were subjected to normal, high-,

Table 2. *Plasma electrolytes in Gpr41 WT and Gpr41 WT mice*

	M, WT	M, KO	F, WT	F, KO	*P* (male)	*P* (female)	*P* (all WT vs. KO)
Na, mmol/l	146.7 ± 0.6	147.8 ± 0.5	148.0 ± 0.7	151.5 ± 1.8	0.22	0.13	0.08
Cl, mmol/l	116.9 ± 1.3	117.8 ± 1.2	113.8 ± 1.4	113.3 ± 0.8	0.62	0.76	0.72
iCa, mmol/l	1.1 ± 0.02	1.2 ± 0.05	1.2 ± 0.03	1.3 ± 0.01	0.42	0.17	0.31
TCO_2, mmol/l	15.3 ± 1.6	15.8 ± 0.8	19.5 ± 0.5	18.5 ± 1.3	0.79	0.47	0.91
Glucose, mg/dl	205.4 ± 11.4	190.9 ± 12.6	179.0 ± 13.0	182.8 ± 12.2	0.41	0.84	0.56
BUN, mg/dl	18.6 ± 1.5	19.4 ± 1.0	19.0 ± 2.6	20.0 ± 1.6	0.65	0.75	0.57
Creatinine, mg/dl	<0.2	<0.2	<0.2	<0.2			
Hematocrit, % PCV	46.0 ± 0.4	45.5 ± 0.7	47.8 ± 0.8	47.0 ± 1.5	0.57	0.67	0.45
Hemoglobin, g/dl	15.6 ± 0.1	15.5 ± 0.2	16.3 ± 0.3	16.0 ± 0.5	0.59	0.65	0.45
Anion gap, mmol/l	21.4 ± 1.0	21.5 ± 1.3	22.0 ± 1.8	24.3 ± 1.8	0.97	0.41	0.59

Blood chemistries of Gpr41 wild-type (WT) and knockout (KO) mice are similar. $n = 7$, male (M) WT, 8 M KO; $n = 4$, females (F). iCa, ionized calcium; TCO_2, total carbon dioxide; BUN, blood urea nitrogen; PCV, packed cell volume.

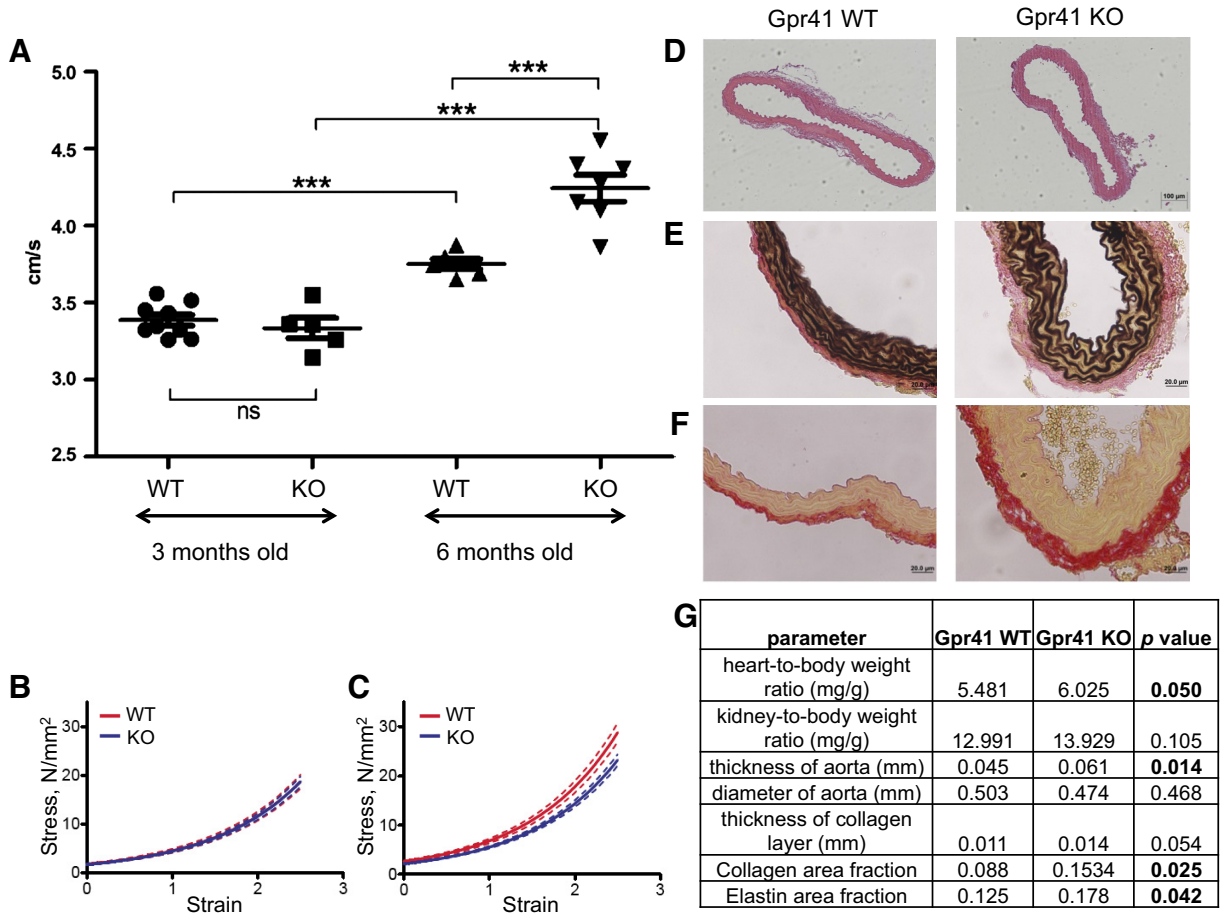

G

parameter	Gpr41 WT	Gpr41 KO	*p* value
heart-to-body weight ratio (mg/g)	5.481	6.025	**0.050**
kidney-to-body weight ratio (mg/g)	12.991	13.929	0.105
thickness of aorta (mm)	0.045	0.061	**0.014**
diameter of aorta (mm)	0.503	0.474	0.468
thickness of collagen layer (mm)	0.011	0.014	0.054
Collagen area fraction	0.088	0.1534	**0.025**
Elastin area fraction	0.125	0.178	**0.042**

Fig. 3. Vessel properties of Gpr41 KO mice. Three-month-old Gpr41 KO and WT mice have similar pulse wave velocities, whereas 6 mo old Gpr41 KO mice have increased pulse wave velocity; $n = 6$, $^{***}P < 0.01$ (*A*). However, the tensile properties of intact Gpr41 KO and Gpr41 WT aortas are similar; $n = 4$ (*B*). In fact, decellularized Gpr41 KO aortas have significantly greater compliance (*C*), $P < 0.0001$. *D–F*: representative images from histology of aortas from Gpr41 WT (*left*) and KO (*right*) mice. Hematoxylin and eosin staining of aortas from 6 mo old Gpr41 WT and Gpr41 KO mice (*D*) show no major histological differences, other than the thickening of aorta in Gpr41 KO mice. Verhoeff's van Gieson staining was used to quantify elastin (black) in 6 mo old Gpr41 WT aortas and Gpr41 WT aortas (*E*). Picrosirius red staining of aortas from 6 mo old male Gpr41 WT, Gpr41 KO (*F*) mice was used to quantify collagen. *G*: quantification of vascular properties of male Gpr41 mice; $n = 4$ (vessel thickness, diameter, collagen, elastin quantification); $n = 6$ (heart and kidney-to-body weight ratios).

and low-salt diets. Systolic hypertension was observed during the dark cycle in Gpr41 KO mice on the salt-matched control diet (0.49% NaCl; different from the control diet used in Fig. 2), similar to our previous observation. Severe hypertension was observed in one Gpr41 KO mouse in this cohort (baseline BP during dark cycle 160/122 mmHg); the data acquired from this animal were excluded from the analyses in Fig. 4. A high-salt diet (4% NaCl) did not affect BP in Gpr41 WT mice, while a minor, nonsignificant increase in systolic pressure was observed in Gpr41 KO mice (~2.6 mmHg, $P = 0.21$ *day 7* of high-salt diet vs. *day 1* of baseline) (Fig. 4*A*, Table 4). Hence, Gpr41 KO mice do not have salt-sensitive hypertension. Diastolic BP and heart rate were similar in Gpr41 KO and WT on the control, high-salt and low-salt diets (Fig. 4, *B* and *C*), although some day-wise comparisons reached significance, particularly daytime diastolic values during low-salt diet. Interestingly, while Gpr41 WT mice exhibit a reduction in systolic pressure on low-salt diet [~5.6 mmHg, $P = 0.03$ (light cycle); −6. 1 mmHg, $P = 0.02$ (dark cycle), *day 3* of low-salt diet vs. average of baseline], this trend is markedly attenuated in Gpr41 KO mice (Table 4, Fig. 4).

Table 3. *Plasma renin concentration in 3-month-old Gpr41 KO and WT male and female mice*

Male, WT	105.94 ± 8.57, n= 7
Male, KO	115.3 ± 16.25, n=7
Female, WT	129.88 ± 5.92, n= 6
Female, KO	139.55 ± 9.87, n= 6

Plasma renin concentration in 3 mo old mice (ng angiotensinogen I produced/ml/h).

DISCUSSION

In this study, we demonstrate that murine Gpr41 localizes to the vascular endothelium, that an intact endothelium is necessary for SCFA-mediated vasodilation, and that Gpr41 KO mice have isolated systolic hypertension. Systolic hypertension in Gpr41 KO appears to be vascular in origin, as it is not associated with changes in plasma renin and is not salt-sensitive. Our studies highlight the rapidly emerging role for gut microbiota to influence host BP regulation and provide a

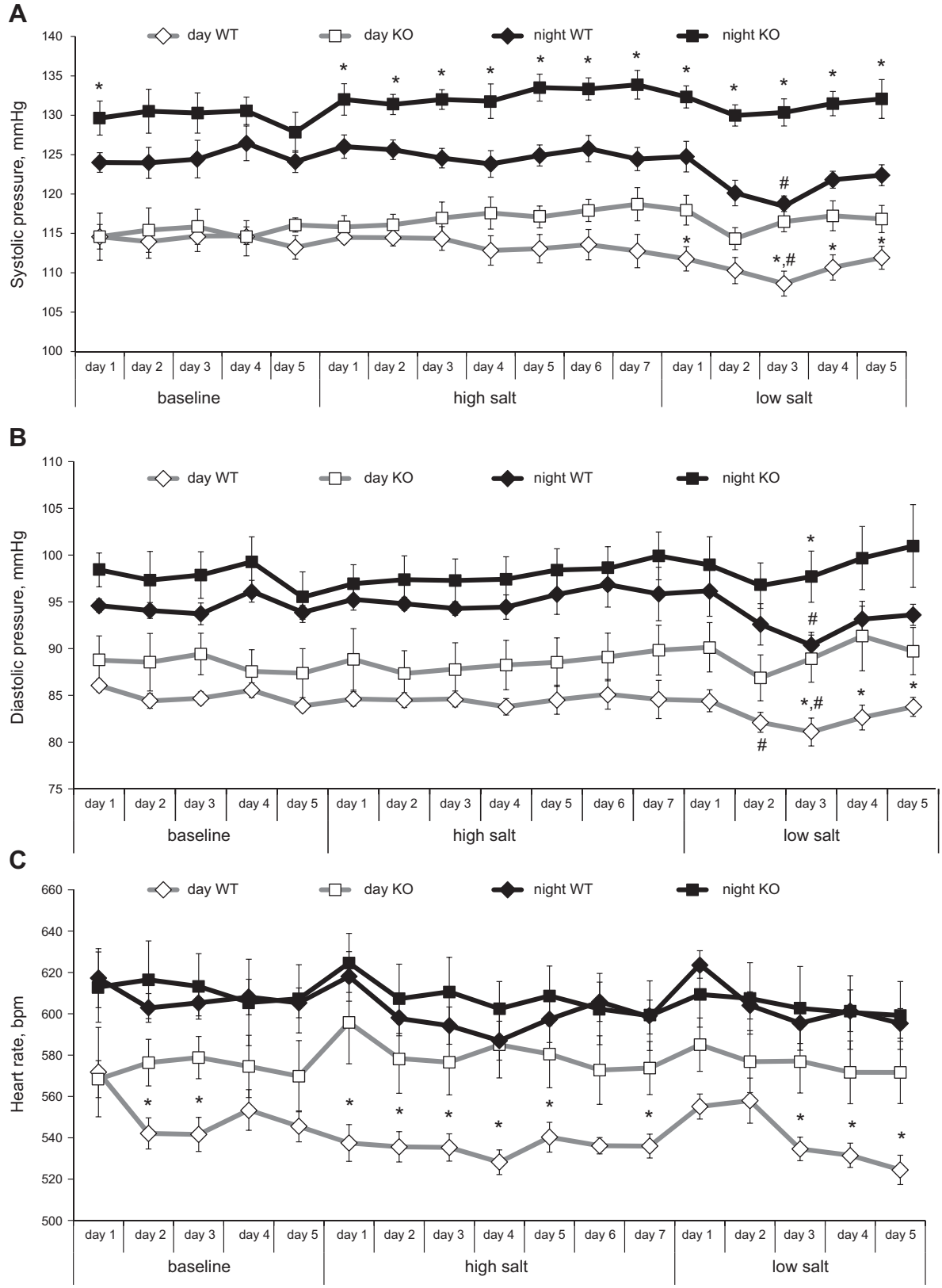

Fig. 4. Gpr41 KO mice do not exhibit salt-sensitive hypertension. *A*: day-wise trends of systolic pressure in Gpr41 KO and WT mice during the salt diet treatment period show the lack of effect of differing salt diets on systolic pressure. Baseline values shown are average systolic blood pressure (BP) values of the 5-day baseline recording period. $n = 6$ (WT), 5 (KO). Day-wise trends of diastolic pressure (*B*) and of heart rate (*C*) on normal, high-salt, and low-salt diets. $*P < 0.05$ between genotypes. $\#P < 0.05$ baseline average vs. indicated day.

Table 4. *Difference in systolic pressure compared with average baseline systolic pressure*

	ΔP (systolic pressure, mmHg)			
	WT, Day	KO, Day	WT, Night	KO, Night
		High salt		
Day 1	0.3 ± 1.1	0.6 ± 1.9	1.4 ± 1.4	2.2 ± 1.9
Day 2	0.2 ± 1.2	0.8 ± 1.5	1.0 ± 1.2	1.6 ± 1.4
Day 3	0.1 ± 0.7	1.7 ± 1.5	−0.03 ± 0.9	2.2 ± 1.1
Day 4	−1.4 ± 1.1	2.3 ± 1.5	−0.8 ± 0.7	2.0 ± 1.3
Day 5	−1.2 ± 0.5	1.8 ± 1.7	0.3 ± 1.1	3.7 ± 1.5
Day 6	−0.6 ± 0.9	2.7 ± 2.6	1.2 ± 1.1	3.6 ± 2.3
Day 7	−1.5 ± 1.2	3.4 ± 3.5	−0.1 ± 1.8	4.1 ± 3.1
		Low salt		
Day 1	−2.5 ± 1.1	2.7 ± 3.3	0.2 ± 1.7	2.6 ± 3.0
Day 2	−3.9 ± 1.4	−0.9 ± 1.4	−4.5 ± 1.6	0.2 ± 1.2
Day 3	−5.6 ± 1.7	1.2 ± 2.8	−6.1 ± 1.7	0.6 ± 2.6
Day 4	−3.5 ± 1.4	2.0 ± 2.9	−2.8 ± 1.5	1.7 ± 2.5
Day 5	−2.3 ± 1.2	1.6 ± 2.4	−2.2 ± 1.0	2.3 ± 3.5

key mechanistic link between microbial metabolites and host physiology.

Role of the endothelium. In our study, we report that Gpr41 localizes to the vascular endothelium. Localization of Gpr41 to the vascular endothelium is consistent with a previous report of Gpr41 in the vascular endothelium of human adipose tissue (2). Given that Olfr78 [another SCFA receptor, with a significantly higher EC_{50} (31)] is found in the vascular smooth muscle, it implies that the vascular response to SCFAs is likely complex and coordinated. Although the vasodilatory response to SCFAs is robust and well documented, SCFA-induced vasodilation was initially reported to be endothelium independent (27) but was more recently shown to be dependent on the endothelium (19) [initial studies were likely misled by the use of SCFA concentrations in excess of 30 mM (1)]. Our studies agree with those of Knock et al. (19), as we find that SCFA-mediated vasodilation is largely endothelium dependent at doses within the physiological range, although in our hands it appears that there may be a smaller vascular smooth muscle component as well. The fact that the ex vivo response to SCFAs is largely dependent upon the endothelium but is not blocked by L-NAME, implies that the mechanism of vasodilation likely involves either endothelium-derived hyperpolarizing factor or prostaglandins (34).

It is important to note that in addition to its localization to the endothelium, Gpr41 has also been reported in the sympathetic nervous system, another cell type that could certainly influence BP. In this previous study (17), it was reported that Gpr41 increased sympathetic drive, and one indicator of altered sympathetic drive in the Gpr41 KO was a decreased resting heart rate. However, in our study we did not measure any change in heart rate at baseline during either the dark or the light cycle. Potential explanations for this discrepancy include the method of measurement (we utilized telemetry, whereas the previous study measured heart rate by tail cuff), as well as the fact that the KO mice used in the two studies were generated by two independent groups. Thus, in our study, we focused on a potential role for endothelial Gpr41 in modulating baseline BP, although we certainly cannot discount potential influences of the sympathetic nervous system.

Salt sensitivity and renin in Gpr41 KO. On a high-salt diet, there is a minor and nonsignificant increase in systolic pressure in Gpr41 KO mice, indicating that these mice do not display classic salt sensitivity. However, Gpr41 KO mice used in this study are on a C57BL/6 genetic background, which is relatively resistant to the development of hypertension upon moderate salt challenge (9); thus, a longer salt-loading may be useful in further evaluating this model. It is also intriguing to note that although C57BL/6 are relatively resistant to salt-sensitive hypertension, the significant decrease in BP observed in Gpr41 WT mice on *day 2* and *3* of low-salt diet (Table 4) may be an indicator of salt sensitivity.

We did not observe changes in plasma renin in Gpr41 KO animals. Although observations that associate isolated systolic hypertension with lowered plasma renin activity levels have been made in elderly populations (8), it has been shown (in a study population with subjects from a broader age range) that patients with isolated systolic hypertension can be classified into three groups based on plasma renin activity: low renin, normal renin, and high renin (24, 25). In a small cohort of mice, we also measured aldosterone-to-renin ratios and likewise did not find differences between genotypes (data not shown). Thus, the isolated systolic hypertension observed in Gpr41 KO mice does not seem to be associated with differential regulation of the renin-angiotensin-aldosterone system.

Vascular hypertension in Gpr41 KO. It is important to note that our studies utilized whole-animal Gpr41 KO, and, as noted above, Gpr41 is expressed in other tissues beyond the vascular endothelium (2, 17, 20, 39, 43). Therefore, it is worth carefully considering which cell or tissue type likely plays the key role in driving the hypertensive phenotype. Classic essential hypertension is characterized by an increase in both systolic pressure and diastolic pressure. An isolated increase in the systolic pressure in Gpr41 KO mice is indicative of a vascular hypertension, driven by stiff, less-compliant blood vessels, which drive an increase in afterload. Indeed, multiple lines of evidence indicate that the hypertension observed in Gpr41 KO is vascular in nature. First, the aforementioned "isolated systolic" nature of the hypertension; second, plasma renin concentration is not different between WT and Gpr41 KO; and finally, the lack of significant salt sensitivity. Although we cannot rule out a potential role for other sites of expression in contributing to the hypertension, the phenotype seen in these mice is certainly consistent with a vascular origin of hypertension. It is intriguing that the mice lacking Gpr41 present with systolic hypertension without a trend in diastolic pressure, given that SCFAs are vasodilatory. Arterial BP, which is affected by both the active and passive characteristics of blood vessels, is regulated at multiple levels by vascular, hormonal, and nervous inputs. Assessment of tensile properties shows no differences in passive blood vessel characteristics between Gpr41 WT and KO animals. In the future, it will be important to better understand how the active characteristics of Gpr41 KO vessels may be altered and to assess vascular reactivity of Gpr41 KO and WT blood vessels to acetylcholine and sodium nitroprusside in order to better understand the changes driving this phenotype. In addition, it will be important to carefully dissect potential roles of Gpr41 in other tissues and cell types (i.e., using tissue-specific KOs) to determine definitely the contributing role of each tissue toward the final phenotype. Intriguingly, in contrast to our findings for Gpr41, we previously reported that the hypotension induced by the loss of Olfr78 is (at least in part) hormonal in nature (lowered plasma renin). Thus, SCFAs

and host GPCRs mediate two different novel BP regulation pathways, making these pathways intriguing future targets for potential intervention.

Vascular function in Gpr41 KO. Our data imply that vascular function is altered in Gpr41 KO mice: not only do Gpr41 KO exhibit isolated systolic hypertension, but PWV is increased at 6 mo of age. We were surprised to find no difference in PWV at 3 mo of age (3 mo old KO mice are hypertensive); it is possible either that the difference in PWV is within the error of our measurement at 3 mo or that PWV truly does not elevate until after hypertension is established. When studying blood vessels ex vivo (6 mo of age), we found that Gpr41 KO and WT mice have similar tensile properties. Thus, we find that at 6 mo of age PWV is increased in Gpr41 KO (measured in vivo), whereas tensile properties of isolated blood vessels (studied ex vivo) are not stiffer. The fact that we observe a difference in vessel stiffness in vivo but not ex vivo implies that the hypertension may not be driven by structural changes in the vessel but, rather, by changes in vascular signaling mechanisms that occur in vivo (i.e., by changes in vascular tone). The fact that Gpr41 KO vessels studied ex vivo are more compliant than WT when decellularized and have an increased elastin component when examined histologically implies that compensatory structural changes to the vessel may actually be attenuating the hypertension in Gpr41 KO. In addition, although we utilized age-matched controls for both the 3 and 6 mo old animals, with older animals we cannot rule out potential secondary effects related to age, and not solely due to the loss of Gpr41.

In this study, we demonstrate the role of an SCFA receptor, Gpr41, in BP regulation. It is important to note that, although not studied here, in addition to SCFAs, β-hydroxybutyrate, a ketone body, may also be a ligand for Gpr41 [it has been reported as both an antagonist of Gpr41 (17) and an agonist for Gpr41 (43)]. It will be important to carefully address potential roles for β-hydroxybutyrate in future studies. In this study, although the increase in systolic pressure in Gpr41 KO animals is somewhat mild, understanding the underlying mechanism behind SCFA-mediated BP regulation is important since Gpr41 mediates a hypotensive response to a microbially produced compound. Based on the magnitude of change in BP upon acute SCFA infusion in our previous report [>10 mmHg at higher doses, (31)] it is crucial to assess the role of Gpr41 in SCFA-mediated hypotension, as Gpr41 and its downstream signaling partners could be potential targets for novel therapeutics to treat hypertension. In addition, better understanding of how host GPCRs respond to microbial metabolites may yield insights into how hypertension develops and progresses. In the future, it will be important to delineate the cell signaling pathways, both in the host and in the microbes, that contribute to BP regulation and to carefully explore how better understanding or perhaps manipulation of these pathways may be used for benefit.

ACKNOWLEDGMENTS

We are very grateful to Dr. Yanagisawa (UT Southwestern) and Dr. Gordon (Washington University) for the kind gift of Gpr41 KO mice.

GRANTS

This work was supported by the American Heart Association (Predoctoral Fellowship to N. Natarajan, 16IRG27260265 to J. L. Pluznick), the National Institutes of Health (R01DK-107726 and R01HL-128512 to J. L. Pluznick) and Japan Heart Association (D. Hori).

DISCLOSURES

No conflicts of interest, financial or otherwise, are declared by the author(s).

AUTHOR CONTRIBUTIONS

N.N., N.A.F., D.E.B., and J.L.P. conception and design of research; N.N., D.H., S.F., and J.S. performed experiments; N.N., D.H., S.F., and J.S. analyzed data; N.N. and J.L.P. interpreted results of experiments; N.N., D.H., S.F., and J.S. prepared figures; N.N. drafted manuscript; N.N. and J.L.P. edited and revised manuscript; N.N., D.H., S.F., J.S., N.A.F., D.E.B., and J.L.P. approved final version of manuscript.

REFERENCES

1. **Aalkjaer C.** Short chained fatty acids and the colon: how do they cause vasodilatation? *J Physiol* 538: 674, 2002.
2. **Brown AJ, Goldsworthy SM, Barnes AA, Eilert MM, Tcheang L, Daniels D, Muir AI, Wigglesworth MJ, Kinghorn I, Fraser NJ, Pike NB, Strum JC, Steplewski KM, Murdock PR, Holder JC, Marshall FH, Szekeres PG, Wilson S, Ignar DM, Foord SM, Wise A, Dowell SJ.** The Orphan G protein-coupled receptors GPR41 and GPR43 are activated by propionate and other short chain carboxylic acids. *J Biol Chem* 278: 11312–11319, 2003.
3. **Chatterjee S, Bedja D, Mishra S, Amuzie C, Avolio A, Kass DA, Berkowitz D, Renehan M.** Inhibition of glycosphingolipid synthesis ameliorates atherosclerosis and arterial stiffness in apolipoprotein E−/− mice and rabbits fed a high-fat and -cholesterol diet. *Circulation* 129: 2403–2413, 2014.
4. **Chotani MA, Flavahan S, Mitra S.** Silent α2C-adrenergic receptors enable cold-induced vasoconstriction in cutaneous arteries. *Am J Physiol Heart Circ Physiol* 278: H1075–H1083, 2000.
5. **David LA, Maurice CF, Carmody RN, Gootenberg DB, Button JE, Wolfe BE, Ling AV, Devlin AS, Varma Y, Fischbach MA, Biddinger SB, Dutton RJ, Turnbaugh PJ.** Diet rapidly and reproducibly alters the human gut microbiome. *Nature* 505: 559–563, 2014.
6. **de La Serre CB, Ellis CL, Lee J, Hartman AL, Rutledge JC, Raybould HE.** Propensity to high-fat diet-induced obesity in rats is associated with changes in the gut microbiota and gut inflammation. *Am J Physiol Gastrointest Liver Physiol* 299: G440–G448, 2010.
7. **De Vadder F, Kovatcheva-Datchary P, Goncalves D, Vinera J, Zitoun C, Duchampt A, Bäckhed F, Mithieux G.** Microbiota-generated metabolites promote metabolic benefits via gut-brain neural circuits. *Cell* 156: 84–96, 2014.
8. **Durukan M, Guray U, Aksu T, Guray Y, Demirkan B, Korkmaz S.** Low plasma renin activity and high aldosterone/renin ratio are associated with untreated isolated systolic hypertension. *Blood Press* 21: 320–325, 2012.
9. **Hartner A, Cordasic N, Klanke B, Veelken R, Hilgers KF.** Strain differences in the development of hypertension and glomerular lesions induced by deoxycorticosterone acetate salt in mice. *Nephrol Dialysis Transplant* 18: 1999–2004, 2003.
10. **Henningsson Å, Björck I, Nyman M.** Short-chain fatty acid formation at fermentation of indigestible carbohydrates. *Food Nutr Res* 45: 165–168, 2001.
11. **Hosseini A, Behrendt C, Regenhard P, Sauerwein H, Mielenz M.** Differential effects of propionate or β-hydroxybutyrate on genes related to energy balance and insulin sensitivity in bovine white adipose tissue explants from a subcutaneous and a visceral depot. *J Anim Physiol Anim Nutr* 96: 570–580, 2012.
12. **Høverstad T, Midtvedt T.** Short-chain fatty acids in germfree mice and rats. *J Nutr* 116: 1772–1776, 1986.
13. **Inoue D, Kimura I, Wakabayashi M, Tsumoto H, Ozawa K, Hara T, Takei Y, Hirasawa A, Ishihama Y, Tsujimoto G.** Short-chain fatty acid receptor GPR41-mediated activation of sympathetic neurons involves synapsin 2b phosphorylation. *FEBS Lett* 586: 1547–1554, 2012.
14. **Intengan HD, Schiffrin EL.** Vascular remodeling in hypertension: roles of apoptosis, inflammation, and fibrosis. *Hypertension* 38: 581–587, 2001.
15. **Kannel WB, Dawber TR, McGee DL.** Perspectives on systolic hypertension. The Framingham study. *Circulation* 61: 1179–1182, 1980.
16. **Kau AL, Ahern PP, Griffin NW, Goodman AL, Gordon JI.** Human nutrition, the gut microbiome and the immune system. *Nature* 474: 327–336, 2011.

17. **Kimura I, Inoue D, Maeda T, Hara T, Ichimura A, Miyauchi S, Kobayashi M, Hirasawa A, Tsujimoto G.** Short-chain fatty acids and ketones directly regulate sympathetic nervous system via G protein-coupled receptor 41 (GPR41). *Proc Natl Acad Sci USA* 108: 8030–8035, 2011.
18. **Kimura I, Ozawa K, Inoue D, Imamura T, Kimura K, Maeda T, Terasawa K, Kashihara D, Hirano K, Tani T, Takahashi T, Miyauchi S, Shioi G, Inoue H, Tsujimoto G.** The gut microbiota suppresses insulin-mediated fat accumulation via the short-chain fatty acid receptor GPR43. *Nat Commun* 4: 1829, 2013.
19. **Knock G, Psaroudakis D, Abbot S, Aaronson PI.** Propionate-induced relaxation in rat mesenteric arteries: a role for endothelium-derived hyperpolarising factor. *J Physiol* 538: 879–890, 2002.
20. **Le Poul E, Loison C, Struyf S, Springael JYY, Lannoy V, Decobecq MEE, Brezillon S, Dupriez V, Vassart G, Van Damme J, Parmentier M, Detheux M.** Functional characterization of human receptors for short chain fatty acids and their role in polymorphonuclear cell activation. *J Biol Chem* 278: 25481–25489, 2003.
21. **Moloney RD, Johnson AC, O'Mahony SM, Dinan TG, Greenwood-Van Meerveld B, Cryan JF.** Stress and the microbiota-gut-brain axis in visceral pain: relevance to irritable bowel syndrome. *CNS Neurosci Ther* 22: 102–117, 2015.
22. **Mortensen FV, Nielsen H, Mulvany MJ, Hessov I.** Short chain fatty acids dilate isolated human colonic resistance arteries. *Gut* 31: 1391–1394, 1990.
23. **Natarajan N, Pluznick JL.** Olfaction in the kidney: 'smelling' gut microbial metabolites. *Exp Physiol* 101: 478–481, 2016.
24. **Niarchos AP, Laragh JH.** Effects of diuretic therapy in low-, normal- and high-renin isolated systolic systemic hypertension. *Am J Cardiol* 53: 797–801, 1984.
25. **Niarchos AP, Laragh JH.** Renin dependency of blood pressure in isolated systolic hypertension. *Am J Med* 77: 407–414, 1984.
26. **Nowicki PT, Flavahan S, Hassanain H, Mitra S, Holland S, Goldschmidt-Clermont PJ, Flavahan NA.** Redox signaling of the arteriolar myogenic response. *Circ Res* 89: 114–116, 2001.
27. **Nutting CW, Islam S, Daugirdas JT.** Vasorelaxant effects of short chain fatty acid salts in rat caudal artery. *Am J Physiol Heart Circ Physiol* 261: H561–H567, 1991.
28. **Padmanabhan S, Caulfield M, Dominiczak AF.** Genetic and molecular aspects of hypertension. *Circ Res* 116: 937–959 2015.
29. **Perry RJ, Peng L, Barry NA, Cline GW, Zhang D, Cardone RL, Petersen KF, Kibbey RG, Goodman AL, Shulman GI.** Acetate mediates a microbiome-brain-beta-cell axis to promote metabolic syndrome. *Nature* 534: 213–217, 2016.
30. **Pluznick JL.** Renal and cardiovascular sensory receptors and blood pressure regulation. *Am J Physiol Renal Physiol* 305: F439–F444, 2013.
31. **Pluznick JL, Protzko RJ, Gevorgyan H, Peterlin Z, Sipos A, Han J, Brunet I, Wan LXX, Rey F, Wang T, Firestein SJ, Yanagisawa M, Gordon JI, Eichmann A, Peti-Peterdi J, Caplan MJ.** Olfactory receptor responding to gut microbiota-derived signals plays a role in renin secretion and blood pressure regulation. *Proc Natl Acad Sci USA* 110: 4410–4415, 2013.
32. **Ramkumar N, Ying J, Stuart D, Kohan DE.** Overexpression of renin in the collecting duct causes elevated blood pressure. *Am J Hypertens* 26: 965–972, 2013.
33. **Ridaura VK, Faith JJ, Rey FE, Cheng J, Duncan AE, Kau AL, Griffin NW, Lombard V, Henrissat B, Bain JR, Muehlbauer MJ, Ilkayeva O, Semenkovich CF, Funai K, Hayashi DK, Lyle BJ, Martini MC, Ursell LK, Clemente JC, Van Treuren W, Walters WA, Knight R, Newgard CB, Heath AC, Gordon JI.** Gut microbiota from twins discordant for obesity modulate metabolism in mice. *Science (New York, NY)* 341: 1241214, 2013.
34. **Rubanyi GM.** Endothelium-derived relaxing and contracting factors. *J Cell Biochem* 46: 27–36, 1991.
35. **Samuel BS, Shaito A, Motoike T, Rey FE, Backhed F, Manchester JK, Hammer RE, Williams SC, Crowley J, Yanagisawa M, Gordon JI.** Effects of the gut microbiota on host adiposity are modulated by the short-chain fatty-acid binding G protein-coupled receptor, Gpr41. *Proc Natl Acad Sci USA* 105: 16767–16772, 2008.
36. **Sekirov I, Russell SL, Antunes LC, Finlay BB.** Gut microbiota in health and disease. *Physiol Rev* 90: 859–904, 2010.
37. **Smith PM, Howitt MR, Panikov N, Michaud M, Gallini CA, Bohlooly YM, Glickman JN, Garrett WS.** The microbial metabolites, short-chain fatty acids, regulate colonic Treg cell homeostasis. *Science (New York, NY)* 341: 569–573, 2013.
38. **Steppan J, Sikka G, Jandu S, Barodka V, Halushka MK, Flavahan NA, Belkin AM, Nyhan D, Butlin M, Avolio A, Berkowitz DE, Santhanam L.** Exercise, vascular stiffness, and tissue transglutaminase. *J Am Heart Assoc* 3: e000599, 2014.
39. **Sykaras AG, Demenis C, Case RM, McLaughlin JT, Smith CP.** Duodenal enteroendocrine I-cells contain mRNA transcripts encoding key endocannabinoid and fatty acid receptors. *PLoS One* 7: e42373, 2012.
40. **Tazoe H, Otomo Y, Karaki SI, Kato I, Fukami Y, Terasaki M, Kuwahara A.** Expression of short-chain fatty acid receptor GPR41 in the human colon. *Biomed Res (Tokyo)* 30: 149–156, 2009.
41. **Ulven T.** Short-chain free fatty acid receptors FFA2/GPR43 and FFA3/GPR41 as new potential therapeutic targets. *Front Endocrinol* 3: 111, 2012.
42. **Wilkinson IB, Franklin SS, Cockcroft JR.** Nitric oxide and the regulation of large artery stiffness: from physiology to pharmacology. *Hypertension* 44: 112–116, 2004.
43. **Won YJJ, Lu VB, Puhl HL, Ikeda SR.** β-Hydroxybutyrate modulates N-type calcium channels in rat sympathetic neurons by acting as an agonist for the G-protein-coupled receptor FFA3. *J Neurosci* 33: 19314–19325, 2013.
44. **Zhou Y, Varadharaj S, Zhao X, Parinandi N, Flavahan NA, Zweier JL.** Acetylcholine causes endothelium-dependent contraction of mouse arteries. *Am J Physiol Heart Circ Physiol* 289: H1027–H1032, 2005.
45. **Zieman SJ, Melenovsky V, Kass DA.** Mechanisms, pathophysiology, and therapy of arterial stiffness. *Arterioscler Thromb Vasc Biol* 25: 932–943, 2005.